

# A 3D Printed Power-Split Device for Testing Energy Management Strategies Applied to Hybrid Vehicles

Jose L. Torres\* Francisco M. Arrabal\*\* Jose L. Blanco\*  
Antonio Gimenez\*

\* *Dpto. de Mecanica, Universidad de Almeria - CIESOL. Campus de Excelencia Internacional Agroalimentario, ceiA3, crta. Sacramento s/n, 04120 Almeria, Spain (e-mail: jltmoreno@ual.es).*

\*\* *Dpto. de Fisica y Quimica, Universidad de Almeria, crta. Sacramento s/n, 04120 Almeria, Spain (e-mail: fmarrabal@ual.es).*

**Abstract:** This work presents a testbed emulating the hybrid electric vehicles powertrain with both teaching and research purposes. The core of this testbed is a 3D printed epicycloidal gearset actuating as a power split device. Its design and hardware equipment are explained as well as its working principle. From an educational point of view, this system states an interesting control problem and, at the same time, exemplifies the operation of this kind of machines with the scope of a motivating application. Consequently, a teaching methodology comprising this testbed is proposed. In addition, the challenging nature of the system encourage the development of optimization techniques aimed at reducing the overall system energy consumption. Results of a preliminary experiment are satisfactory addressed. As a consequence, the presented testbed is proposed as a remote lab for teaching and benchmarking new control strategies.

© 2015, IFAC (International Federation of Automatic Control) Hosting by Elsevier Ltd. All rights reserved.

*Keywords:* Hybrid vehicles, Motor control, Differential gears, Computer interfaces, Energy management system.

## 1. INTRODUCTION

Environmental cost of mobility is becoming a global problem in recent years. Electric vehicles are called to be a good alternative to conventional cars powered by internal combustion engines. However, some considerations have to be taken into account. At high scale, the  $CO_2$  reduction as a consequence of the use of electric vehicles is strictly affected by the technology employed in the generation of electricity. Moreover, the limited autonomy of full-electric vehicles may suppose a handicap to this alternative, see Torres et al. (2014) for a comparative study. As an intermediate term, Hybrid Electric Vehicles (HEVs) are playing a key role nowadays aimed at reducing the emissions of  $CO_2$  as a consequence of human and goods transportation, see Liu and Peng (2008). Among the benefits of the hybridization of vehicles it is not only count with propulsion machines using different sources of energy but also being able to operate near the optimal point of each one, as discussed in Torres et al. (2014). Mechanically, this is achieved by means of a power-split device (PSD). This element comprises the core of the powertrain in a HEV. In most cases, these kind of devices are composed by a planetary gear set and a series of electro-mechanical clutches, as described in Lin et al. (2003). Other cases, these systems include continuously variable transmission (CVT) applying for both cars, see Miller (2006) and motorcycles, see Chung and Hung (2014). Yeo et al. (2006) In Yeo et al. (2006), this device is considered as an interesting agent in the recovery of energy during decelerations. Regarding the

$CO_2$  emissions reduction and energy saving, the management of PSDs require accurate control strategies, see Liu and Peng (2006). This problem has been studied during the two last decades, see Brahma et al. (2000); Lin et al. (2003) for an example. More recently, in Borhan et al. (2012), a model predictive control strategy is employed for this purpose, with satisfactory results. Currently, this problem still remains being a challenging research field. In Sciarretta et al. (2014), a benchmark is presented dealing with this topic.

The literature review carried out in this work reveals that most of the related studies are addressed exclusively through simulations. Among the commercial tools focused on this subject, ADVISOR, presented in Markel et al. (2002), arises as one of the most frequently employed. The investment needed for real experiment is quite expensive. This is the idea beyond this work. On the one hand, having a prototype of a PSD enlarges the number of experiments aimed at validating new control strategies. On the other hand, the PSD is a clear example of a planetary gearset which can be used as a complementary testbed for subjects such as Theory of Machines and Mechanisms, since most students have difficulty visualizing the gears motion in these systems. At the same time, this prototype exemplifies the use of this kind of mechanism to a real-world problem, which, moreover, results attractive for engineering students from different disciplines. It is also worth to remark that planetary gear sets are been recently employed in research of new applications, i.e. variable stiffness actuators for service robotics, as presented in

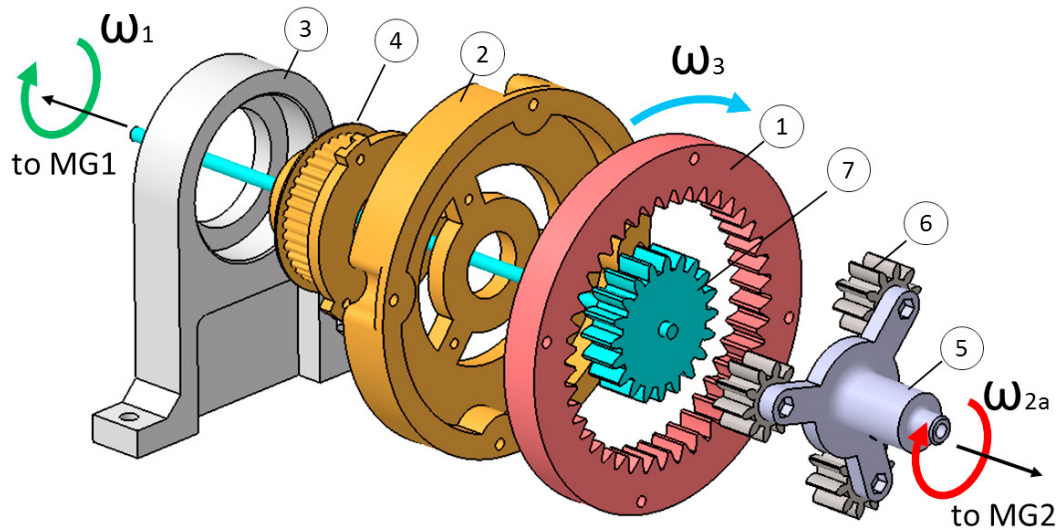


Fig. 1. Exploded view of the planetary gear system. The angular of the sun gear, the carrier and the ring are represented by  $\omega_1$ ,  $\omega_{2a}$  and  $\omega_3$  respectively.

Groothuis et al. (2014); Kim et al. (2010), or mobile robotics, see Lee and Choi (2012) for an example.

The theoretical approach employed in this work for managing our PSD prototype is based on the use of *nomographs*. This technique, applied to HEVs, will be discussed in depth, as well as the use and construction of a nomograph. It is straightforward to implement graphically in the GUI developed in this work as SCADA tool for managing the complete testbed this way of graphically represent the kinematic relations involved in the attached problem.

This paper is structured as follows: First, technical aspects of the prototype developed in this work are explored in section 2, along with its working principle. Then, a teaching exercise is proposed in section 3. Afterwards, in section 4 an experiment is performed as an example of the 3D printed power-split device (3D-PSD) operation is addressed, and preliminary results are presented. Finally, conclusions of this work are presented in section 5.

## 2. THE 3D-PSD

In this section, we present the 3D-PSD in detail, its working principle and the targets behind the prototype. The core of the system is an epicycloidal gearset. According to Fig. 1, the ring gear (1) is a  $Z_r=40$  teeth inner gear with an external diameter of 144 mm. This component is attached to a main case (2) which is inserted into a bearing placed on a bracket (3) fixed to the ground. A pulley (4) which is also attached to the case allows to transfer the motion of the ring gear to a parallel axle. The transmission is carried out by means of a belt and another pulley, performing a 44/14 ratio. This axle allows to easily introduce loads into the systems as well as to measure the output angular speed ( $\omega_3$ ) by means of a rotatory incremental encoder. The carrier link (5) consists of another 3D printed part which is connected to the motor-generator MG2. This link contains the axles of the three planet gears (6), of  $Z_p=10$

teeth each. The sun gear (7) is connected to the motor-generator MG1, placed in opposition to the main case by means of a metallic axle. Consequently, the number of teeth of the sun gear is  $Z_s=20$ . Both motor-generators, from now on referred to as DC-motors (MG1 and MG2), are connected to the ground by two supports made on stainless steel. Thus, a two degrees of freedom planetary gear system is obtained, whose outputs are the angular speeds of the carrier and sun gear, and the input is the desired angular speed of the ring gear when operating in automatic mode.

Fig. 2 shows the real testbed. The two DC-motors employed labeled *MG1* and *MG2* correspond with the DC-motors of the manufacturer Pololu with a reduction gear of 100:1 and a 64 pulses per revolution (ppr) encoders. The encoder which registers the ring speed (*ENC*), is an optical

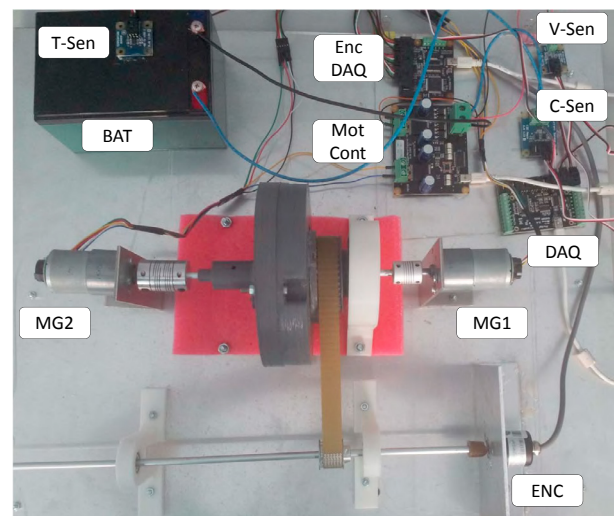


Fig. 2. Complete system and hardware description.

rotary encoder ISC3004, by Hedss, and performs 1200 ppr. In order to read both the encoders of each DC-motor and the ISC3004 encoder, a PhidgetEncoder Highspeed 4-Input Data Acquisition Board (*Enc DAQ*) is connected to a laptop via USB. The laptop also controls the two DC-motors simultaneously by means of a PhidgetMotorControl HC (*Mot Cont*). A 12V/10Ah battery (*BAT*) model 6-CNFJ-10 by Lead Crystal actuates as power supply. In order to measure the total energy consumed by the system, two additional sensors are employed. The first one is a Phidgets precision voltage sensor (*V-Sen*) which registers the battery voltage. The second one is an Phidgets 30 A current sensor AC/DC (*C-Sen*) which measures the current passing from the battery to the motors controller. Signals from both sensors as well as the battery temperature registered by the Phidgets precision temperature sensor (*T-Sens*) are processed by PhidgetInterfaceKit 8/8/8 Data Acquisition Board (*DAQ*) connected to the laptop via USB. The software architecture developed for this purpose is based on the APIs provided by Phidgets, upon a .NET framework.

### 2.1 Working Principle

Following the discussion in Torres et al. (2014), the main objective of a PSD focuses on combining two or more sources of motion. In this work, two motors are connected to the sun gear and the carrier respectively as exposed before. This configuration is based on a simplified version of commercial hybrid vehicles powertrain.

For the sake of simplification, the internal combustion engine (ICE) and the clutches typically employed in these kind of systems are removed. Moreover, generator (which usually operates connected to the ICE) is treated as a simple DC-motor. From now on, this component will be referred to as MG2, and will be related to the carrier angular speed,  $\omega_{2a}$ . On the other hand, the motor connected to the sun gear is another identical DC-motor referred to as MG1, with an angular speed  $\omega_1$ . Finally, the system output is the ring angular speed,  $\omega_3$ , when operating in manual mode. The kinematic relation between these three velocities is expressed as follows:

$$\rho = \frac{\omega_3 - \omega_{2a}}{\omega_1 - \omega_{2a}} \quad (1)$$

Where  $\rho = -Z_s/Z_r$  represents the apparent gear ratio, that is, the gear ratio when considering the system as an ordinary gear train (the carrier link is blocked). Hence, the ring angular speed is obtained as:

$$\omega_3 = \omega_1 \cdot \frac{1}{1 - \rho} - \omega_{2a} \cdot \frac{1 - \rho}{\rho} \quad (2)$$

Since this equation counts with two independent variables, each operating point could be obtained, in theory, from and infinite number of combinations of  $\omega_1$  and  $\omega_{2a}$ . According to this criterion, this system is considered as a Single Input Multiple Output (SIMO) system.

With the motion of the planetary gear train fully defined, it becomes important to understand the torque requirements of the system. This has traditionally been achieved by a static force analysis of a specific gear train. While this is a valid technique, it requires the selection of a specific planetary arrangement, and it is an error-prone

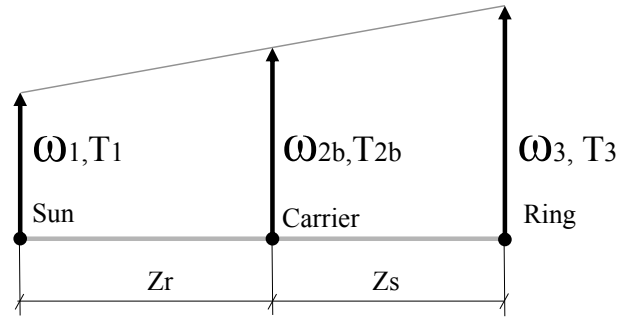


Fig. 3. Nomograph employed in modeling our power-split device.

and extensive computational process. Instead, it is simpler to use the principle of energy conservation. The energy balance equation for the general planetary gear train can be written as:

$$T_1\omega_1 + T_{2b}\omega_{2a} + T_3\omega_3 = 0 \quad (3)$$

Where  $T_i$  represent the torques applied to each branch of the gear train. The careful selection of two specific cases for  $\omega_1$  and  $\omega_3$  will quickly yield equations completely defining the torques on the three branches of the gear train.

The first case to examine is the instance when the gear train is moving as solid axle, that is  $\omega_1 = \omega_{2a} = \omega_3 = \omega$ . In this case, Equation (3) can be rewritten as:

$$T_1\omega + T_{2b}\omega + T_3\omega = 0 \quad (4)$$

Collecting terms and assuming  $w$  is non-zero, it can be quickly deduced that:

$$T_1 + T_{2b} + T_3 = 0 \quad (5)$$

This is first of two equation that will define the torque requirements of the planetary gear train.

The second case of interest is that of zero speed at the carrier. Using (2) and substituting zero for  $\omega_{2a}$ . Hence:

$$\omega_3 = \rho\omega_1 \quad (6)$$

Making this substitution and substituting zero for  $\omega_{2a}$  in (3):

$$T_1\left(\frac{1}{\rho}\omega_3\right) + T_3\omega_3 = 0 \quad (7)$$

Again, collecting terms and rearranging into a more convenient form, the second torque governing equation is found to be:

$$T_3 = -T_1\frac{1}{\rho} \quad (8)$$

Using this equation, along with (5), one can fully characterize the torque requirements at any two branches of the gear train, given the torque at the remaining branch.

Once this analysis is completed, the system has been reduced to the solution of the equations (2), (5), and (8), involving a total of seven variables. While this seems to imply that the designer has free choice of any four variables, the torque equations are independent of rotational speed. This means that the designer must select one torque, along with either three speeds or two speeds and a gear ratio. With so many variables being selected by the engineer, it become important to be able to visualize the response of the design to changes in any of these variables. A suitable approach when dealing with this kind of problems consist of elaborating a *nomographs*, as depicted in Fig. 3.

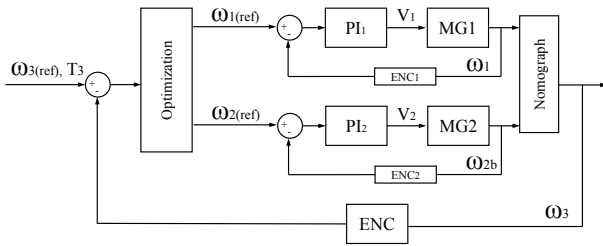


Fig. 4. Control loop of the entire system.

This procedure leads to an intuitive interface for a first understanding of the attached problem.

### 2.2 Overall plant control strategy

The control problem may be represented by the control loop depicted in Fig. 4, where the optimization problem attends to the criterion of motors operation point. It has been stated that there are infinite operating points that may satisfy a determined output requirement. However, it is convenient to discuss about some issues:

- Kinematic constraints that has to be accomplished according to (2).
- Torque and speed limitations of the motors.
- Efficiency of the complete plant.

Whereas the two first constraints are mandatory, the level of efficiency of the overall plant depends on the selected operating point of each DC-motor analyzed independently. This issue comprises an interesting optimization problem. As mentioned in the introduction of this work, high efforts are made in researching new optimization and control rules in order to maximize the efficiency of HEV. In our 3D-PSD, this efficiency mainly depends on the performance of the DC-motors. Hence, the energy management strategy to considers must include two layers. The first one may be considered as the high-level control layer. This layer is the responsible of selecting an optimal setpoint to each DC-motor which satisfies the ring angular speed requirements. At this stage, the efficiency of each DC-motor under this conditions is considered. Afterwards, a low-level control loop has to be implemented in order to each DC-motor reaches the speed demanded in the high-level layer.

### 2.3 DC-motors parameters and control

According to the data provided by the manufacturer, it has been considered two identical DC-motors featuring 11000 rpm, 300 mA free-run, 0.3 kg · cm and a stall  $i_s = 5 A$  at a rated voltage of  $v_{in} = 12 V$ . The resistive term of the motor, which can also be measured experimentally, is  $R_m = 2.4 \Omega$ . Neglecting the motor armature inductance, the models employed in this work are simplified to first order transfer functions.

In order to control each motor independently, PI controllers are designed by using the Ziegler Nichols method in closed loop, in which the proportional constant is obtained from the critic constant that converts the plant output to an oscillating signal, and the critic time is considered the period of such oscillations.

## 3. PROPOSED TEACHING METHODS

The testbed developed in this work presents a problem of control suitable for undergraduate students. This problem deals with two topics which are studied in depth in any engineering curriculum, such as electric motors and epicycloidal gears. Whereas the utilization of DC-motors is frequently employed as laboratory material, it is not so common to count with a completely monitorized planetary gearset. Moreover, the combination of these elements presented in this work are related to an interesting field of study, as the case of hybrid vehicles, boosting the students' motivation. As mentioned in previous sections, the proposed control problem may be solved, from a kinematic point of view, by a broad number of solutions. However, when considering the energy consumption, an optimization problem arises. Hence, it maybe performed a benchmark in which the students, in addition to solve the kinematic problem controlling properly the DC-motors, are encouraged to minimize the overall system energy consumption.

All these features make our proposed 3D-PSD a good tool for teaching several engineering subjects. Even when its overall cost is not excessive, this prototype will be treated as a remote laboratory in a first stage. Other remote labs have successfully been employed in related courses, as the quadruple-tank model presented in Pasamontes et al. (2012). A schedule of the tasks to deal with when using the 3D-PSD in a teaching exercise is presented next:

### 3.1 Characterize the DC-motors.

The students are encouraged to obtain their transfer functions from the constants provided by the manufacturer, along with real input-output data are provided as ground-truth. Parameter identification techniques maybe applied additionally.

### 3.2 Control each motor independently.

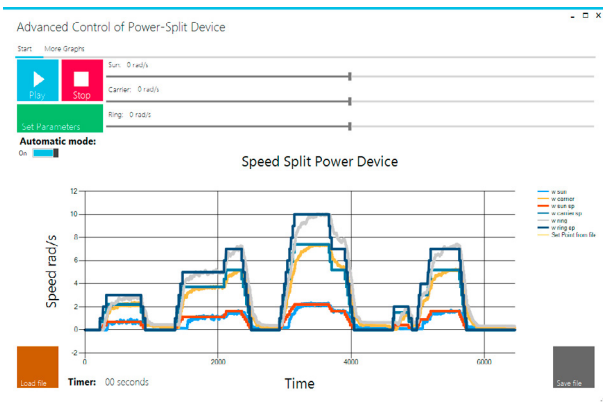
Once the DC-motors are modeled correctly, any valid controller may be developed. For the sake of simplicity, a PI controller is proposed. Its constants should be obtained according to a known technique, as the Ziegler-Nichols method employed in Section 2.3.

### 3.3 Verify the ring speed in open loop mode.

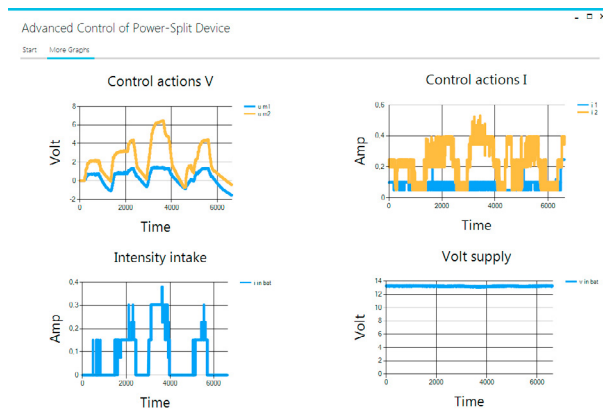
At this stage, the students are able to set any arbitrary speed to each DC-Motor. This may be performed in the real system as follows: (i) the controller constants are introduced to the SCADA tool, (ii) the *operating mode option* in the SCADA tool is switched to *manual* and (iii) the sliders corresponding to each DC-motor are taken to the position corresponding to the desired velocity. The depending velocity, that is, the ring angular speed, is then read in the SCADA tool. This velocity is compared to that obtained by the students by hand calculations following the recommendations presented in Section 2.1.

### 3.4 Correct the phenomena that make mismatch the results

The system considered is a clear example in which the backlash of the gearings has to be taken into account.



(a) Software interface main menu and angular velocities.



(b) Power consumptions.

Fig. 5. Example experiment and preliminary results.

Moreover, some additional issues must be analyzed, such as signals noise or system delays.

### 3.5 Set a rule for close the loop of the complete system.

This task corresponds with the criterion to be established for achieving the ring angular velocity from the respective velocities of MG1 and MG2. At this stage, the *mode* option is switched to *automatic* in the SCADA tool, and the sliders belonging to the DC-motors remain inactive. Instead, a third slider bar allows to set the desired angular speed of the system reference. The DC-motors velocities, as well as their power consumption and the total power provided by the battery are shown in each time step.

### 3.6 Test the control strategy in a normalized cycle.

At this stage, the high level control law should have been validated for discrete and manually set ring gear velocities references. Then, in this task, the students are encouraged to test their proposed control laws during a complete cycle. For this purpose, with the *mode* option switched to *automatic* in the SCADA tool, a text file corresponding to desired cycle must be loaded. The cycles are selected from a database, and represent real standard driving which are adjusted to be performed in the 3D-PSD. The main analysis to carry out is to check how the ring speed fit to the required velocity.

### 3.7 Perform an energy consumption analysis.

In each complete cycle experiment, dataset registering all the signals involved are grabbed. With this information, the students are able to analyze the operating point of each DC-motor during the entire cycle, as well as the amount of energy provided by the battery. Then, results are compared among the participants, and new control strategies can be addressed in order to reduce the energy consumption without losing velocity and acceleration performance.

This practice takes into account some of the paradigms stated by the Bologna Process, which was implemented in all the Engineering degrees of the University of Almeria in 2010. Concretely, the proposed practical activity is a clear example of Problem Based Learning (PBL). This activity is scheduled to be carried out during the second semester of the third academic year of the Industrial Engineering degree, in the subject of Computer Control (6 ECTS). This subject is mandatory for the specialty in Electronics and optional for the specialties in Chemistry and Mechanics. At this stage, all the students have coursed the subjects of Theory of Machines and Mechanisms and Industrial Automation, so they are familiarized with the mechanical problem involving the planetary gearset and have an appropriate knowledge of Control Theory.

The proposed methodology must accomplish two hours of autonomous work focused at the characterization of the motors and the design of a controller. Afterwards, a practical session must be carried out so that the student may verify and correct their models. This task corresponds to a laboratory session of two hours, in which groups of three students will operate the testbed in turns of 10 minutes each group. Then, in another session of autonomous work with duration of 2 hours, the students must define a control law for performing the entire closed-loop system, and test the results for a normalized cycle through simulations. Finally, in a second laboratory session, the students will test their control strategy in the real testbed, and their results in term of consumption and performance will be compared among the other groups.

## 4. PRELIMINARY EXPERIMENTS AND RESULTS DISCUSSION

In order to demonstrate the operation of the 3D-PSD, a preliminary experiment is performed. As a first criterion of decision for determine the operating point of the DC-motors, the angular speed of the sun gear ( $\omega_1$ ) is imposed to remain proportional to the carrier link angular speed ( $\omega_{2b}$ ). Thus, the control law follows an arbitrary rule such as  $\omega_1 = 0.3\omega_{2b}$ . As a consequence the value of the ring angular speed  $\omega_3$  is determined according to Equation 2. This strategy does not take into account any optimization law. However, it is possible to evaluate the accuracy of the low-level control layer in which each DC-motor is controlled in order to perform a determined ring angular velocity. Moreover, preliminary energy considerations may be addressed. The input for this experiment is based on normalized profiles of velocities typically employed in the automotive sector, such as the New European Driving Cycle (NEDC). Fig. 5 shows the results of this experiment. In Fig. 3.6, the reference and the ring angular velocity

are represented as well as the angular velocities of MG1 ( $\omega_1$ ) and MG2 ( $\omega_{2b}$ ) along with their respective setpoints. On the other hand, Fig. 3.6 show the values of voltage and current which are necessary to compute the power consumed by each DC-motor as well as power provided by the battery.

In order to develop a remote lab from the presented testbed, some guidelines has been considered. For this purpose, the student will be assigned a schedule table provided by the professors, performing an authorization system based on a specifically developed software programmed in .NET. In addition, data base is designed so that contains all necessary information namely the students' name, access date, season time, user name and password. Firstly the student executes the application and a form containing basic fields to get access to remote lab must be correctly fulfilled. If all conditions are satisfied, a TCP/IP connection with a specific socket among the client application and the server raises up. Finally, the client application is connected by an asynchronous mode that means a string is sent to the server when occurs an event. The server is also a daemon application with a *select case* function which reads the string sent and proceeds according to that string. Both client and server are programmed in .NET.

## 5. CONCLUSIONS

In this work, a testbed to be employed as a remote lab is presented. This testbed, based on a epicycloidal gearset referred to as 3D-PSD equipped with a series of sensors and actuators has been explained in detail. The theoretical framework and the 3D-PSD working principle has been related to the key points to cover when using this testbed with teaching purposes. Afterwards, an example of experiment has been performed. Results show the correct operation of all the sensors and actuators employed in the testbed. As a future work, the testbed will be connected to a server in order to allow its remote operation. Moreover, more sophisticated control laws will be employed, taking into account the DC-motors efficiency with the aim to be extrapolated to real hybrid electric vehicles.

## 6. ACKNOWLEDGMENTS

This work has been partially funded by the Spanish "Ministry of Economy and Competitiveness" under the contracts DPI 2011-22513 and DPI2014-56364-C2-1-R as well as by the Andalusian Regional Government grant programs FPDU 2009 and the excellence project P12-FQM-2668, co-funded by the European Union through the European Regional Development Fund (ERDF).

## REFERENCES

- Borhan, H., Vahidi, A., Phillips, A., Kuang, M., Kolmanovsky, I., and Di Cairano, S. (2012). Mpc-based energy management of a power-split hybrid electric vehicle. *Control Systems Technology, IEEE Transactions on*, 20(3), 593–603. doi:10.1109/TCST.2011.2134852.
- Brahma, A., Guezennec, Y., and Rizzoni, G. (2000). Optimal energy management in series hybrid electric vehicles. In *American Control Conference, 2000. Proceedings of the 2000*, volume 1, 60–64. IEEE.
- Chung, C.T. and Hung, Y.H. (2014). Energy improvement and performance evaluation of a novel full hybrid electric motorcycle with power split e-cvt. *Energy Conversion and Management*, 86(0), 216 – 225. doi: <http://dx.doi.org/10.1016/j.enconman.2014.04.043>.
- Groothuis, S., Rusticelli, G., Zucchelli, A., Stramigioli, S., and Carloni, R. (2014). The variable stiffness actuator vsaut-ii: Mechanical design, modeling, and identification. *Mechatronics, IEEE/ASME Transactions on*, 19(2), 589–597. doi:10.1109/TMECH.2013.2251894.
- Kim, B.S., Song, J.B., and Park, J.J. (2010). A serial-type dual actuator unit with planetary gear train: Basic design and applications. *Mechatronics, IEEE/ASME Transactions on*, 15(1), 108–116. doi: 10.1109/TMECH.2009.2019639.
- Lee, H. and Choi, Y. (2012). A new actuator system using dual-motors and a planetary gear. *Mechatronics, IEEE/ASME Transactions on*, 17(1), 192–197. doi: 10.1109/TMECH.2011.2165221.
- Lin, C.C., Peng, H., Grizzle, J., and Kang, J.M. (2003). Power management strategy for a parallel hybrid electric truck. *Control Systems Technology, IEEE Transactions on*, 11(6), 839–849. doi:10.1109/TCST.2003.815606.
- Liu, J. and Peng, H. (2006). Control optimization for a power-split hybrid vehicle. In *American Control Conference, 2006*, 6 pp.–. doi:10.1109/ACC.2006.1655400.
- Liu, J. and Peng, H. (2008). Modeling and control of a power-split hybrid vehicle. *Control Systems Technology, IEEE Transactions on*, 16(6), 1242–1251. doi: 10.1109/TCST.2008.919447.
- Markel, T., Brooker, A., Hendricks, T., Johnson, V., Kelly, K., Kramer, B., OKeefe, M., Sprik, S., and Wipke, K. (2002). Advisor: a systems analysis tool for advanced vehicle modeling. *Journal of Power Sources*, 110(2), 255 – 266. doi:[http://dx.doi.org/10.1016/S0378-7753\(02\)00189-1](http://dx.doi.org/10.1016/S0378-7753(02)00189-1).
- Miller, J. (2006). Hybrid electric vehicle propulsion system architectures of the e-cvt type. *Power Electronics, IEEE Transactions on*, 21(3), 756–767. doi: 10.1109/TPEL.2006.872372.
- Pasamontes, M., Álvarez, J.D., Guzmán, J.L., and Berenguel, M. (2012). Learning switching control: A tank level-control exercise. *IEEE Transactions on Education*, 55(2), 226–232. doi:10.1109/TE.2011.2162239.
- Sciarretta, A., Serrao, L., Dewangan, P., Tona, P., Bergshoeff, E., Bordons, C., Charmpa, L., Elbert, P., Eriksson, L., Hofman, T., Hubacher, M., Isenegger, P., Lacandia, F., Laveau, A., Li, H., Marcos, D., Nesch, T., Onori, S., Pisu, P., Rios, J., Silvas, E., Sivertson, M., Tribioli, L., van der Hoeven, A.J., and Wu, M. (2014). A control benchmark on the energy management of a plug-in hybrid electric vehicle. *Control Engineering Practice*, 29(0), 287 – 298. doi: <http://dx.doi.org/10.1016/j.conengprac.2013.11.020>.
- Torres, J.L., Gonzalez, R., Gimenez, A., and Lopez, J. (2014). Energy management strategy for plug-in hybrid electric vehicles. A comparative study. *Applied Energy*, 113, 816–824. doi:10.1016/j.apenergy.2013.08.007.
- Yeo, H., Hwang, S., and Kim, H. (2006). Regenerative braking algorithm for a hybrid electric vehicle with cvt ratio control. *Proceedings of the Institution of Mechanical Engineers, Part D: Journal of Automobile Engineering*, 220(11), 1589–1600.